RSS-based Ranging by Leveraging Frequency Diversity to Distinguish the Multiple Radio Paths

Yunhuai Liu, *Member, IEEE,* Dian Zhang*, *Member, IEEE,* Xiaonan Guo, *Member, IEEE,*
Min Gao, *Member, IEEE,* Zhong Ming, *Member, IEEE,* Lei Yang, *Member, IEEE,*
and Lionel M. Ni, *Fellow, IEEE*

Abstract—Among various ranging techniques, Radio Signal Strength (RSS) based approaches attract intensive research interests because of its low cost and wide applicability. RSS-based ranging is prone to be affected by the multipath phenomenon which allows the radio signals to reach the destination through multiple propagation paths. To address this issue, previous works try to profile the environment and refer this profile during run-time. In a practical dynamic environment, however, the profile frequently changes and the painful retraining is needed. Rather than such static ways of profiling the environments, in this paper, we try to accommodate the environmental dynamics automatically in real-time. The key observation is that given a pair of nodes, the RSS at different spectrum channels will be different. This difference carries the valuable phase information of the radio signals. By analyzing these RSS values, we are able to identify the amplitude of signals solely from the Line-of-Sight (LOS) path. This LOS amplitude is a simple function of the path length (the physical distance). We find that the analysis is a typical non-linear curvature fitting problem that has no general routing algorithms. We prove that, this problem format is ill-conditioned which has no stable and trustable solutions. To deal with this issue, we further explore the practical considerations for the problem and modify it to a greatly improved conditioning shape. We solve the problem by numerical iterations and implement these ideas in a real-time indoor tracking system called MuD. MuD employs only three TelosB nodes as anchors. The experiment results show that in a dynamic environment where five people move around, the averaged localization error is about 1 meter. Compared with the traditional RSS-based approaches in dynamic environments, the accuracy improves up to 10 times.

Index Terms—Pervasive computing, wireless sensor networks, ranging, RSS, frequency diversity, multiple radio paths, dynamic environment.

---

1 INTRODUCTION

Ranging plays an essential role in indoor localizations [2], [18], [14], [4]. Among the various techniques, one promising approach is based on Radio Signal Strength (RSS). Nodes simply measure the RSS in between and map the RSS values to the corresponding distances. Compared with other ranging techniques, RSS-based ranging offers many unique advantages. It requires little hardware support and can be implemented with any wireless transceivers. Most off-the-shelf wireless devices support real-time RSS measurements, making the RSS nearly a free resource for ranging. Because of these advantages, RSS-based ranging (and localizations) has attracted a vast amount of research efforts and is the hottest topic

in literature (e.g., [2], [36], [35], [34], [10]).

As RSS measurement is easy and convenient, the mapping from RSS to distances is the key issue. In theory, this mapping is a unique and monotonous function. For example, the free-space path loss model [21] suggests that the RSS path loss is proportional to the square of the distance. In practice, however, this model is far from reality. It has been well known that this function is a dynamic and complex one that depends on many factors [21], and the most significant one is the multipath propagation phenomenon [2].

In wireless communications, multipath phenomenon refers to the nature of radio propagation that radio signals reach the receiver along two or more physical paths. There are many causes such as the atmospheric duct, refraction and reflection. Signals from different paths combine at the receiver constructively or destructively depending on signal phases. As the phases are environment-dependent, the RSS of combined signals is very sensitive to the environment changes. Fig. 1 depicts some real RSS measurements for a pair of telosB nodes [1] under different distances at different places. Apparently, there is no simple unique function between the RSS and the corresponding distance.

In order to find an appropriate mapping between

- *Yunhuai Liu is with the Third Research Institute of Ministry of Public Security, P.R. China. E-mail: yunhuai.liu@gmail.com.*
- *Dian Zhang and Zhong Ming are with College of Computer Science and Software Engineering, Shenzhen University, P.R. China. E-mail: serena.dian@gmail.com, mingz@szu.edu.cn.*
- *Xiaonan Guo, Min Gao are with the Department of Computer Science and Engineering, the Hong Kong University of Science and Technology. E-mail: guoxn@ust.hk,mingao@ust.hk,ni@cse.ust.hk.*
- *Lei Yang, Lei Yang are with the Faculty of Information Technology, the Macau University of Science and Technology. E-mail: leiyang@must.edu.mo.*

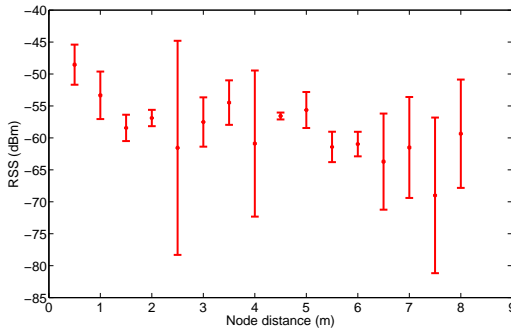* *Dian Zhang is the corresponding author and the jointed first author.*
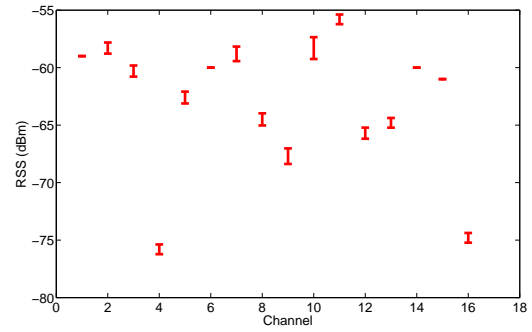
Fig. 1. RSS measurement in different environments

Fig. 2. RSS measurement in different channels: node distance$= 2m$

the RSS and the distance, a large amount of research works have been conducted. The fundamental way in the above approaches is to profile the radio environment and refer the profile when ranging. Representative works include RADAR [2], LANDMARC [19], statistic approaches [25], and etc. [18], [14], [4]. Profile-based approaches require a labor-intensive training procedure to provide the environment profile, which is too costly and becomes practically infeasible when the environment changes fast (e.g., people moving around). This limitation greatly weakens the advantages of RSS-based ranging, making people reluctant to apply it in real environments.

Revisiting the multipath effect, we argue that a more fundamental way to deal with this issues is to accommodate the environmental dynamics in real time. We attempt to accomplish this by distinguishing the signals from different paths, filtering out signals from the Non-Line-Of-Sight paths (NLOS) and identifying the one from the Line-Of-Sight path (LOS). Therefore, the multipath effect can be eliminated. The main advantage is that we focus only on the RSS values which requires no additional hardware support or other lower-layer protocol information than the RSS. To the best of our knowledge, this is the first work in literature towards this goal with such constraints.

To achieve this goal is extremely difficult because of the limited information provided by RSS. RSS measures merely the signal amplitude and provides no signal phase information. Signals from different paths may exhibit similar behaviors from the RSS's perspective. For example, RSS of a LOS path may be exactly the same as that of a short but reflected path. Moreover, using common hardware, we have no direct measurement on the NLOS paths.

An interesting observation is that the frequency diversity may help to provide phase information indirectly. Fig. 2 depicts some RSS measurements for a pair of TelosB sensors at different spectrum channels (the frequency ranging is from $2.4 - 2.4835GHz$ and the band is divided into 16 channels with $22MHz$). We can see that, the pair of nodes may have significantly different RSS values at different spectrum channels and the measurements are quite stable. This RSS difference at different channels is essential for our work as it carries the valuable phase information. By carefully analyzing these RSS information, we will be able to identify the amplitudes and phases of signals from each path, and derive the accurate distance according to the amplitude of LOS signals. A clearer illustrative example is presented in Sec. 2.3.

We find that the analysis of RSS values is also difficult. It is a typical non-linear curvature fitting problem with trigonometric model functions. It has no close-form solutions and is typically approximated by numerical iterations. We also find that the original fitting problem has a bad shape. Its Hessian matrix is ill-conditioned and the solutions will be un-stable and not trustable, which may yield great ranging errors.

To deal with this issue, we further explore the practical considerations to refine the problem. For example, certain hardware-dependent parameters, though unknown, will be unlikely to change and can be obtained in prior to the ranging. The LOS path is always the shortest path, and reflection will absorb a lot of signal energy. Considering these facts, we design techniques to solve this problem. Based on these treatments, the reformed problem has greatly improved conditioning and the solutions become much more stable.

To demonstrate the effectiveness of this ideas, we implement a real tracking system called MuD (Multipath Distinguishing). It is based on TelosB [1] platform. Compared with the traditional RSS-based ranging and localization, MuD offers the following key advantages. 1) It is robust to the environment dynamics. Moving people, new furniture etc. will not degrade its performance unless the LOS path is affected (e.g., blocked); 2) No labor-intensive training is needed. The training of hardware-oriented parameters is a one-time operation and can be done in an online manner. We can also use values in the hardware specification manual to assign these parameters, which will sacrifice about 10% accuracy; 3) Ranging in MuD is very accurate in dynamic environments. Therefore three

anchor nodes for trilateration purposes are enough for localizations. Our method has the general applicability to all the RSS-based ranging, localization and even gesture recognition [37]. Experimental results show that the average ranging and localization error is about 1 meters in complex and dynamic environments (five people moving around). Compared with the traditional RSS-based approaches in dynamic environment, the accuracy is improved by about 10 times.

The rest of this paper is organized as follows. Sec. 2 gives some background information. Sec. 3 gives the system model and the problem definition. Sec. 4 shows how to use non-linear optimization to solve the above problem. Sec. 5 presents the our solution techniques to improve the problem conditioning. We will describe the implementation of MuD tracking system and evaluate its performance in Sec. 6 and Sec. 7. Sec. 8 will be about related work, followed by discussion. At last, conclusion and future work are given.

2 MULTIPATH EFFECT AND FREQUENCY DIVERSITY

In this section, we provide some background for the multipath effect. We first introduce physical properties of the radio propagations in free space, then describe how the signal behaves in multipath phenomenon. At last we use a simple example to illustrate how to exploit the frequency diversity to eliminate multipath effects. More details of the radio propagation characteristics can be found in physics references. Some notations used in this paper are summarized in Table 1.

2.1 Radio Propagation in Free Space

Radio propagation describes the behavior of radio waves when they are transmitted from the transmitters to the receivers. During the propagation, radio waves will fade out with the distance. In free space, the fading obeys the inverse-square law. The signal strength is proportional to the inverse of the square of the distance between the transmitter and receiver. By Friis model [21] it can be expressed as

$$|\overrightarrow{p}| = \frac{P_t G_t G_r \lambda^2}{(4\pi d)^2} \qquad (1)$$

where $\overrightarrow{p} = \{|\overrightarrow{p}|, \theta\}$ is the signal wave vector, $|\overrightarrow{p}|$ is its amplitude and θ is its phase at the receiver, P_t is its phase at the receiver, G_t and G_r are the antenna gain of the transmitter and receiver, λ is the signal wavelength, and d is the LOS path length and also the physical distance between the transmitter and receiver.

Suppose the sender has the phase zero, then the signal phase at the receiver is

$$\theta = (\frac{d}{\lambda} - \lfloor \frac{d}{\lambda} \rfloor) \cdot 2\pi \qquad (2)$$

TABLE 1
Notations used in this paper

Notation	Description
m	The number of channels that can be used for RSS measurements; in TelosB standard, $m = 16$ from $2.4G - 2.4835G$
λ_j	The wavelength of the j-th channel signals
n	The number of radio propagation paths between the transmitter and receiver
$|\overrightarrow{p_i}|$	The amplitude of the signals along the $i - th$ path to the receiver, called path strength, $i = 1, \ldots, n$
θ_i	The phase of the signals along the $i - th$ path to the receiver, called path phase
$\overrightarrow{p_i}$	$\overrightarrow{P} = \{|\overrightarrow{P_i}|, \theta_i\}$ the signal wave vector along the $i - th path$
d_i	The length of the $i - th path$, $i = 1, \ldots, n$
c	A hardware-dependent constant, $c = p_t G_t G_r$ where p_t is the transmitting power, G_t is the transmitter antenna gain and G_r is the receiver antenna gain
Γ_i	Reflection coefficient of the i-th path
$P(x, \lambda)$	The RSS model function, defined as the absolute value of the sum of the signal vectors from all paths, i.e., $P(x, \lambda) = \| \sum_{i=1}^{n} \overrightarrow{p_i} \|$
x	$x = \{c, \Gamma_2, \ldots, \Gamma_n, d_1, \ldots, d_n\} \in \Re^{2n}$ is the vector of unknown parameters in the model function $P(x, \lambda)$; x is iteratively approximated, $x^{(k)}$ is the $k - th$ iteration value of x and x^* is the final solution
P_j	The RSS measurement at $j - th$ channel
$r_j(x)$	The residual of the RSS measurement and the model function, $r_j(x) = P(x, \lambda_j) - P(j)$
$f(x)$	The least square curvature fitting function defined as $f(x) = \frac{1}{2} \sum_{j=1}^{m} (r_j(x)^2)$ $\bigtriangledown f$ is its first-derivative gradient and $\bigtriangledown_2 f$ is the second-derivative Hessian.

In the remainder of this paper, we call $|\overrightarrow{p}|$ the *path strength*, and θ the *path phase*. For signals along the LOS path, the Friis model is appropriate to describe its behavior as there is no other fading. For NLOS paths in a multipath scenario, we need more physical laws. Note that $\lfloor \rfloor$ is the floor operator.

2.2 Multiple NLOS Paths

The NLOS paths between the transmitter and receiver are mainly induced by reflection, refraction and scattering. There is another kind of diffraction path, which rarely occurs in a common environment. Reflection refers to a radio propagation phenomenon that changes in direction of the signal waves at an

interface between two different media. It results in the returned wave to the original medium. In the indoor environments, the reflections typically occur at the surface of the objects, walls, and the ground. In each reflection, partial energy will be transmitted, partial will be reflected and the left will be absorbed by the medium. The reflectance part is measured by the *reflection coefficient* Γ which is the ratio of the strength of the reflected radio wave E^- to the strength of the incident wave E^+, i.e.,

$$\Gamma = \frac{E^-}{E^+} \qquad (3)$$

With (1) and (3), for a given NLOS path, its path strength is

$$|\overrightarrow{p}| = \Gamma \frac{P_t G_t G_r \lambda^2}{(4\pi d)^2} \qquad (4)$$

Notice that d now is the length of NLOS path and not equal to the distance between the transmitter and receiver. The expression of path phase is similar to (2).

Refraction is another source of the NLOS paths. It has a similar effect on the path strength while this time the transmittance part of the energy rather than the reflected part will be received by the receiver. The path phase is the same as (2).

Scattering is also a source of the NLOS paths. Radio are forced to deviate from a straight trajectory by one or more paths due to localized non-uniformities in the medium through which they pass. It is a kind of diffuse reflection.

According to these physical properties, given a pair of nodes in a static environment, when signals of one channel propagate along a set of paths, very likely the signals of a nearby channel will propagate along the same set of paths. It is because the reflection and refraction are mainly characterized by the wavelength of the signal and nearby channels have a similar wavelength. For example, TelosB nodes [1] work on $2.4G$ band to $2.4835G$ band. The wavelengths are $0.125m$ to $0.1208m$. The difference is only 4.7 millimeters. Thus, The possibility that the existing paths will disappear or new paths will emerge is very small.

2.3 Motivation Example

Although RSS is the average value of the small scale effects, RSS itself carries no phase information. However, when we slightly change the channel, the RSS value will be different. Such information potentially carries the corresponding phase information.

For each path, its path phase will change when the signal frequency changes. For the example in Fig. 3, suppose the length of path a is $2m$. The $2.4G$ signal will have the path phase

$$\theta_a(\lambda_1) = \left(\frac{d_a}{\lambda_1} - \lfloor \frac{d_a}{\lambda_1} \rfloor\right) \cdot 2\pi = \left(\frac{2}{0.125} - \lfloor \frac{2}{0.125} \rfloor\right) \cdot 2\pi = 0$$

The $2.48G$ signal will have the path phase

$$\theta_a(\lambda_2) = (16.5 - 16) \cdot 2\pi = \pi$$

The changed path phase, called *phase-shift* with respect to the path a is

$$\triangle\theta_a = \theta_a(\lambda_2) - \theta_a(\lambda_1)$$

The phase-shift depends on the path length d. It is not directly measurable by commodity hardware.

A key observation which motivates this work is that we can measure the consequence of this phase-shift. In detail, we can measure the consequence of this phase-shift - the different RSS (Fig. 2) at different channels, and infer the phase-shift by analyzing these different RSS. More specifically, suppose the length of another path b in Fig. 3 is $3m$, its phase-shift will accordingly be

$$\triangle\theta_b = \theta_b(\lambda_2) - \theta(\lambda_1) = \frac{3}{0.121} - \frac{3}{0.125} = 1.6\pi$$

The phase-shifts with respect to different paths are different ($\triangle\theta_a \neq_\triangle \theta_b$). These different phase-shifts will change the constructive and destructive relations between signals from different paths. In Fig. 3, at λ_1, the signals from a and b are completely constructive, while at λ_2, the signals from the two paths become somehow destructive. This changed relation will result in a changed RSS measurement. As there are a limited number of paths, and each path introduces a limited number of unknown parameters, we can solve all the unknowns with a sufficient number of RSS measurements at different channels. Indeed, as we will show later, each path will introduce two new unknowns. The current $2.4G$ Zigbee compliance supports up to 16 channels. Therefore it can accommodate up to 8 paths between a pair of transmitter and receiver.

3 PROBLEM DEFINITION

The basic idea of our RSS-based ranging is to let nodes collect the RSS measurements of different spectrums, then make a calculation based on these measurements. However, we will show that it is difficult to analyze, which motivate us to do further design. In this section we first introduce the system model, then formally define the problem.

3.1 System Model and Assumptions

We assume transmitters and receivers are able to adjust their frequency in run time. This function is supported by most products. Each pair of transmitter and receiver are well coordinated and synchronized.

For a given pair of transmitter u and receiver v, suppose there are n radio propagation paths between them (n is unknown). Without loss of generality, let the first path be the LOS one and others be NLOS. The path lengths of these data paths are denoted as
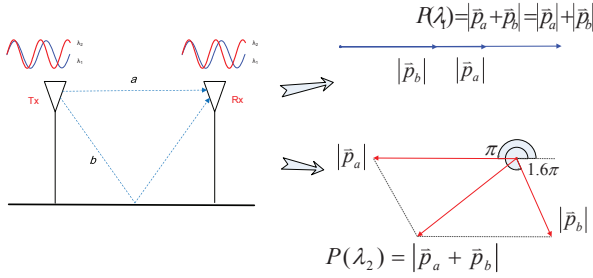
Fig. 3. An illustrative example; there are two paths a and b; The signals of two frequencies λ_1, λ_2 will have different RSS values at the receiver end because of the phase-shift difference between paths (i.e.,$P(\lambda_1) \neq P(\lambda_2)$)

$d_i, i = 1, \ldots, n$ (an accurate d_1 is our ultimate goal). The reflection co-efficiencies of paths are denoted as Γ_i ($\Gamma_1 = 1$ for LOS path and the Γ_i values for other paths are smaller than 1). Suppose by hardware constraint we can measure up to m channel RSS and the wavelengths of these channels are $\lambda_j, j \in [1, m]$. Given the wavelengths λ_j of one channel, we denote the $i - th$ path strength as $p_i(\lambda_j), i \in [1, n]$ and the $i - th$ path phase as $\theta_i(\lambda_j), i \in [1, n]$. During the measurement, we will use the same transmission power P_t (though again it is unknown). For the given pair of transmitter and receiver, the antenna gain G_t and G_r are fixed. We can substitute all the constants P_t, G_t and G_r in (4) with a single one $c = \frac{P_t G_t G_r}{(4\pi)^2}$. Thus we have the $i - th$ path strength as

$$p_i(\lambda_j) = \frac{\Gamma_i c \lambda_j^2}{d_i^2} \qquad (5)$$

and the path phase

$$\theta_i(\lambda_j) = (\frac{d_i}{\lambda_j} - \lfloor \frac{d_i}{\lambda_j} \rfloor) \cdot 2\pi \qquad (6)$$

Considering the different path phases, the aggregated signal at the receiver is a vector summation. Given wavelength λ_j, the RSS the amplitude of the combined signal is

$$
\begin{aligned}
P(x, \lambda_j) &= |\sum_{i=1}^{n} \vec{p_i}| \\
&= ((\sum_{i=1}^{n} c\lambda_j^2 d_i^{-2} \sin(d_i \lambda_j^{-1}))^2 \\
&+ (\sum_{i=1}^{n} c\lambda_j^2 d_i^{-2} \cos(d_i \lambda_j^{-1}))^2)^{\frac{1}{2}} \quad (7)
\end{aligned}
$$

Here we apply the orthogonal decomposition method to calculate vector summations. Equ. (7) is a function $P(x, \lambda_j)$: $\Re^{2n} \rightarrow \Re$ with $x =$

$(c, \Gamma_2, \ldots, \Gamma_n, d_1, \ldots d_n) \in \Re^{2n}$ be the vectors of unknown parameters, or simply the unknowns. $\Re$ is the set of real numbers.

3.2 Problem Definition

For each $j - th$ channel, we will have a RSS measurement $P_j, j \in [1, m]$. More specifically, in Eq. (7) the parameters λ_i, P_j and c are known, while T_i and d_i are unknown. There are m measurements and our main task is to fit these m measurements (λ_j, P_j) with the *model function* $P(x, \lambda_j)$, $x \in \Re^{2n}$. We need to find x so that the fit is as close as possible to the real measurements P_j. We define the "closeness"of the fitting as the least square, and other norms of vectors are also possible when they are well justified. Formally, the problem is defined as **Curvature Fitting Problem (CFP)**:

$$given \ r_j(x) : \Re^{2n} \rightarrow \Re, j = 1 \ldots m$$

$$min_{x \in R^{2n}} f(x) = \frac{1}{2} \sum_{j=1}^{m} r_j(x)^2 \qquad (8)$$

where $r_j(x) = P(x, \lambda_j) - P_j (j = 1, \ldots, m)$ is the individual fitting error, $P(x, \lambda_j)$ is the model function defined in (7).

As long as the problem is solved, the solution, denoted as x^*, will contain our target d_1.

4 NON-LINEAR OPTIMIZATIONS TO SOLVE CFP

In this section, we will show that the present CFP is not in a good shape and has no trustable and stable solution by its current form. In the next, we will first present the intuition of this claim based on the concepts of condition number, then present a general method of solving non-linear equations for CFP. At last, we will show that the solution for the current CFP is based on ill-conditioned matrix.

4.1 Condition Number of Ill-conditioned Matrix

The intuition of this claim is that, the model function $P(x, \lambda)$ is managed by parameters co-efficiency c and path length d_i. Roughly speaking, the trigonometric part (i.e., sines and cosines) in $P(x, \lambda)$ "oscillates" the function value and can be considered as a scalar between 0 and 1. The $\frac{c}{d_i^2}$ portion controls the amplitude and is the dominance part. However, these two parameters c and d_i jointly control the function value and will cancel the effects of each other. For example, a doubled estimation of d_i will cancel the effect of a four time c, resulting a similar function value.

Mathematically, such situations are called $ill-$ $conditioned$ and its degree of the condition is measured by the *condition number*. A high condition number means, a small change in the input will result in

a large change in the solution. For instance, a matrix of condition number 100 will have 100% changes on the solution when the input has 1% changes. Solutions based on this high condition number matrix can hardly be trusted as there are always certain errors on the input in practice.

4.2 General Method for Non-linear Minimizations

In this subsection, we provide some general information of solving non-linear minimizations for CFP. More details can be found in multivariable calculus references [7].

In CFG, the solutions exist only when $m \geq 2n$, the unknowns $x \in \Re^{2n}$ are no more than m model function equations.

Definition: A continuous function $f : \Re^{2n+1} \to \Re$ is said to be continuously differentiable at $x \in \Re^{2n+1}$, if $(\frac{\partial f}{\partial x_i})$ $i \in 1, \ldots, 2n+1$ exists and is continuous; the gradient of f at x is then defined as

$$\nabla f(x) = [\frac{\partial f}{\partial x_i}(x), \ldots, \frac{\partial f}{\partial x_{2n+1}}(x)]^T$$

where $(\frac{\partial f}{\partial x_i})$ is the first partial derivative of f with respect to the $i - th$ variable x_i.

Definition: The Hessian of $f : \Re^{2n+1} \to \Re$ at is defined as the $(2n+1) \times (2n+1)$ matrix whose i, j element is

$$\nabla^2 f(x)_{ij} = \frac{\partial^2 f(x)}{\partial x_i \partial x_j}, i \leq 2n+1, j \leq 2n+1$$

where $\frac{\partial^2 f(x)}{\partial x_i \partial x_j}$ is the second partial derivative of f with respect to the variables x_i and x_j.

Lemma: Let $f : \Re^{2n+1} \to \Re$ be continuously differentiable in an open convex set $D \in \Re^{2n+1}$. Then $x \in D$ can be a local minimizer of f only if $\nabla f(x) = 0$.

Theorem: Let $f : \Re^{2n+1} \to \Re$ be twice continuously differentiable in the open convex set $D \in \Re^n$, and assume there exists $x \in D$ such that $\nabla f(x) = 0$. if $\nabla f^2(x)$ is positive definite, then x is a local minimizer of f.

According to these Lemmas and Theorems, the essential of CFP is then to solve the equations

$$\nabla f(x) = 0$$

or equivalently,

$$\frac{\partial f}{\partial x_i}(x) = 0, i = 1, \ldots, 2n. \tag{9}$$

and among all the solutions to find the one with the minimal $f(x)$.

Since the model function $P(x, \lambda_j)$ involves trigonometric function, (8) are non-linear equations. We can find only approximation solutions and there is no routine algorithm to solve it. This is mainly due to the classical results of no close-form solutions for such problems. Typically the solutions are approximated by numerical iteration. We start the iteration from an initial guess, say $x^{(0)}$, construct a local model for the target function and calculate a new guess, say $x^{(1)}$. The iteration continues until certain criteria are satisfied, e.g., the number of iterations exceeds a given threshold or the consequent approximations are close enough, say $\|\nabla f(x^{(k)})\| \leq \varepsilon$ for an arbitrarily small number ε. This final iteration approximate is then the solution, i.e., $x^* = x^{(k)}$.

4.3 Ill-conditioned Matrix

Applying the Newton's method to (9) we have the iteration equation

$$x^{(k+1)} = x^{(k)} - (\nabla^2 f(x^{(k)}))^{-1} J(x^{(k)})^T R(x^{(k)})$$

where $J(x) \in \Re^{m \times 2n}$ is the Jacobian matrix of f,

$$J_{ji}(x) = \frac{\partial f}{\partial x_i}(\lambda_j), j = 1, \ldots, m; i = 1, \ldots, 2n$$

and $H(x) = \nabla^2 f(x)$ is the second derivatives

$$H(x) = \sum_{j=1}^{m} (\nabla r_i(x) \cdot \nabla r_i(x)^T + r_i(x) \cdot \nabla^2 r_i(x))$$

As the general form of f is too complex that the analytic derivatives $J(x)$ and $H(x)$ are hardly to be available, we just give an analysis on the simplest case where $n = 1$ and $m = 2$ (i.e., there is only the LOS path). We will show that even for this simplest case the problem may still be ill-conditioned.

Theorem: the condition number of Hessian matrix $\nabla^2 f$ with $m = 2$ and $n = 1$ is $(\frac{9c^2}{d_1^2} + 4)^2$

PROOF. For this case, the model function is

$$P((c, d_1,), \lambda_j) = \frac{c\lambda_j^2}{d_1^2}$$

The first derivatives of f is

$$\nabla f = [\lambda_1^2 d_i^2 - 2c\lambda_j^2 d_1^{-3}]$$

and its second derivatives Hessian of f can be described as

$$H = \nabla^2 f = \begin{bmatrix} 0 & -2\lambda_j{}^2 d_1^{-3} \\ -2\lambda_j{}^2 d_1{}^{-3} & 6c\lambda_j{}^2 d_1{}^{-4} \end{bmatrix}$$

The inverse of H is

$$H^{-1} = adj(H)/det(H)$$

where $adj(H)$ adjugate matrix of H and $det(H)$ is the determinant of H. Since H is a rank-2 symmetric matrix, its inverse H^{-1} has the same l_2-norm as the H with a scalar $det(H)^{-2}$. Here the l_2-norm is defined as

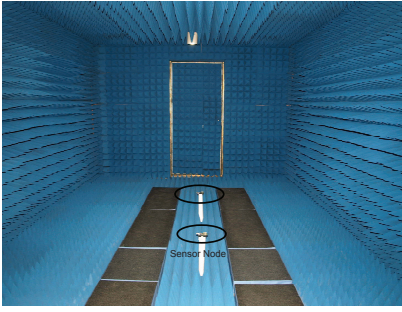$$\|H_2\| = (\sum_{i=1}^{n} \sum_{j=1}^{n} (h_{ij})^2)^{\frac{1}{2}}$$

Fig. 4. Chamber environments

It is used to compute the condition number of H as

$$
\begin{aligned}
Cond(H) &= \|H\|_2\|H^{-1}\|_2 \\
&= det(H)^{-2}(\|H\|_2)^2 \\
&= \frac{1}{16}(\lambda^{-4}d^6)^2((6c\lambda^2 d^{-4})^2 + 2(2\lambda^2 d^3)^2)^2 \\
&= (9\frac{c^2}{d^2} + 2)^2 \qquad\qquad (10)
\end{aligned}
$$

Based on this theorem, we have the following two critical observations. On one hand, for the original format of CFP, the condition number can be arbitrary high when $\frac{c}{d}$ is high enough. For the NLOS paths, we will have a similar conclusion and by substituting the product of c and Γ_i. On the other hand, when we can give a tight bound of these parameters, the condition number can be low, making the matrix well-conditioned, So the solutions are trustable.

5 TREATMENTS OF PROBLEM

In this section, we will present some practical treatments to solve CFP. We first introduce the basic idea of the treatment, then describe them in details.

5.1 Basic Idea of Treatments

By previous section, we find the original CFP can hardly be solved in its current form because of multiple local optimal solutions in the target function f. In addition, the analytic form of the iteration equations is too complex to derive, making the iteration quite hard. It is particularly true for scenarios of more paths, say $n = 8$. Though mathematicians have their means for such situations, their treatments are often investigated in a case-by-case manner. There are yet no effective general-purpose methods to do so.

Rather than those purely mathematic ways, in this paper we attempt to address the issue by practical considerations. Observing the model function $P(x, \lambda)$ in (7), we find that the difficulties of the problem origin from three facts. First, the parameter c, Γ and d jointly affect the function value. The effect of varying one parameter can be canceled by varying the other two parameters for a path. Second, the model function

(7) is symmetric in terms of the different paths. We may be able to find the parameters c and d_i, but can hardly identify which parameters belong to the LOS. Additional information is needed to identify these parameters. Third, the number of paths n is critical to the problem complexity. To accommodate one more path, we have two more unknowns (Γ and d), need at least two more RSS measurements, and two more nonlinear equations. Too complex iteration equations may also aggravate the computation errors due to limited computer precisions. The computation will be greatly simplified if we can limit the number of paths n in calculation, though n indeed is determined by the environments. In the next, we will present how to exploit these observations to simplify CFP.

5.2 Derivation of Fixed Unknowns

A first treatment technique of the problem is to derive some unknowns in the model function. In the model function $P(x, \lambda)$ (Equ. (7)), c represents the co-efficiency $\frac{P_t G_t G_r}{(4\pi)^2}$. For a given pair of transmitter and receiver and a fixed level of the transmission power, c is a constant unknown. We can apply c to the model function, which will dramatically improve the conditioning of the CFP. Therefore, we propose three methods to obtain an estimation of c before the run-time ranging, namely by hardware specifications, by chamber training, and by online training.

5.2.1 Hardware Specification Manuals

Recall the definition of the unknown c, it is determined by the transmission power P_t, and antenna gains of the transmitter G_t and receiver G_r. P_t can be transferred from the power level setting in transmission (e.g., $1dbm \approx 1.26mw$), and G_t and G_r can be obtained from the hardware specification manual (e.g., use the parameter from TelosB datasheet and use the common approach to estimate the gain of omnidirectional antenna [28], [3]). Though this method provides a poor estimation on c, it is the simplest one and sets a baseline for comparison.

5.2.2 Chamber Training

Chambers are enclosures for researchers to investigate the radio propagation phenomenon. Pyramidal absorber materials are deployed to the ceilings, walls and ground in the enclosure to absorb the addition radio waves. Chamber can be considered as an ideal open space where the Friis model is valid. Fig. 4 shows the picture of the chamber that we use in our experiments.

Experiments in chambers are well controlled. As the path length is available, there is only one unknown in the model function $P(x, \lambda)$. Thus for a given pair of transmitter, receiver and the fixed transmission power, we can calculate c by a single RSS measurement.

Chamber is an ideal environment and we set it as the upper limit of the accuracy. In practice, the chamber is often too bulky and may not always available for simple ranging and localization applications.

5.2.3 Online Training

In practical environments, a more attractive option to obtain the parameter c is by online manner.

Specifically, initially the transmitters and receivers will be placed at given positions. With known d_1, we can apply the general method in Sec. 4 to obtain the other unknowns which include c. In detail, actually the procedure of the online training is much similar to the procedure to solve the CFP problem in Section 4. In Section 4, we need to estimate d_1 with known c value. In online training, we need to estimate c with known d_1. The other procedure is the same. In practice, we will deploy the wireless nodes with known distance. It is not required to deploy them the same as in the run-time. For example, users may deploy them in a line with $1m$ apart. This value of c is a one-time calculated value. It will not change as the environment changes. During the later run-time, we apply this c for calculations.

Online training is quite convenient as it requires no chamber equipment. The training procedure shares the same environment as the later ranging and localization procedures, though certain degree of the accuracy will be scarified. We will evaluate these approaches in later sections.

5.3 Reducing the Model Path Number

Another critical parameter in the model function $P(x, \lambda)$ is the number of paths n. It will determine the fundamental form of the function. This parameter is fully environment-dependent and can be any number, and thus brings great challenges to solve CFP.

Nevertheless, in real environment, some practical considerations allow us to set a conservative n (say $n = 5$) without sacrificing too much ranging accuracy.

First, NLOS paths with three or more reflections, refractions, scattering can be ignored. Diffractions rarely occur in a common environment. Recall the radio physical properties that after each reflection, refraction or scattering the path strength will fade according to the reflection co-efficiency Γ. For typical materials, Γ is around 0.5 or less depending on the directional property of the surface [12]. In other words, each reflection, refraction or scattering will consume more than 50% of the energy that can be received by the receiver. More energy will be consumed for the scattering paths. For each NLOS path, more than 87.5% of the energy will be consumed, if the times of reflections, refractions or scattering are more than 3. With over 87.5% of loss on its energy, signals from more than three reflections, refractions or scattering can be ignored in the model function to simplify the

CFP complexity, while it is at the price of certain degree of inaccuracy.

Second, we can also ignore the paths which are extremely long, say more than two times of the LOS path. Recall the Friis model in (1), the energy will fade inversely proportional to the square of the path length. A NLOS path more than twice of the LOS one can have the strength at most one fourth. Considering the further impact of reflection/refraction (Γ), the path energy will be no more than $0.25 \times 0.5 = 0.125$ of the LOS path energy.

Because of these considerations, we set a relatively small n in the model function $P(x, \lambda)$, say $n \leq 5$. Apparently certain accuracy on ranging will be sacrificed. In later section we will use experiments to evaluate the parameter n.

5.4 Bounding the Unknowns for NLOS Paths

Another important issue is the initial value of iterations when we solve CFP. Basically, Newton's method is quite effective when the initial setting is close enough to the solution. Owning to this property, we are motivated to find the upper bound and lower bound of the unknowns. As the target is continuously tracked, the position displacement of the target will not be large due to the limited mobility in the indoor environments. So we heuristically set the upper bound and lower bound of the new d_1 as the original one plus ± 1 meter.

For the NLOS paths, because of the second consideration in the last subsection, their length will be bounded within d_1 and $2d_1$, i.e., $d_1 < d_i < 2d_1$, $i = 2, \ldots, n$. By the physical laws of the radio reflections, we have $\Gamma < 0.3$ for NLOS paths.

5.5 Bounding the Used Channels

In our method, the solution to the CFP Problem exists only when $m \geq 2n$, which means the number of the channels should larger than 2 time of the number of assumed paths. Since we have already assumed that the number of radio propagation paths is 5 (as introduced in the 5.3 subsection), this number of used channel should be larger or equal than 10. So this value is the lower bound. It means that, at least we should utilize 10 channels in the real experiment. Since the number of channels is limited by 16 for the telosB nodes, we use all of them in our experiment. Considering other devices may be chosen for users, we will leave the upper bound of the performance in our future work.

5.6 Summary of the Treatments

With all these treatment techniques, the conditioning of the CFP will be greatly improved. In general, the parameter c is a given number no more than 0.1. By practical deployments the path lengths are no
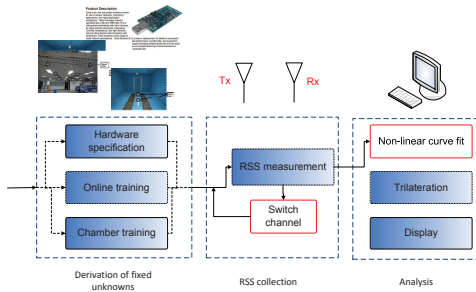
Fig. 5. Architecture of MuD with three major steps: derivation of the fixed unknown c, RSS collection and analysis
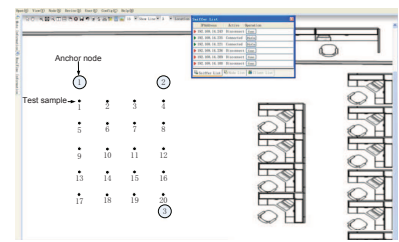
Fig. 6. RSS Experiment environment

Fig. 7. A bird-view snapshot of experiment environment

less than 1 meter (transmitters are deployed on the ceiling). For the single path scenarios, the condition number (8) is no more than $(9 \times 0.1^2 + 2)^2 < 5$ which can be considered as well-conditioned. For multiple paths, because of the reflection co-efficiency Γ, the LOS path energy will be the dominance factor and thus the condition number will also be restrained to an acceptable level.

6 EXPERIMENT

Integrating all these treatments, we implement a RSS-based tracking system called MuD. In this section, we first introduce the architecture, followed by practical challenges and implementation of MuD. Notice that all our experiments are conducted in dynamic environments by default where several people typically five) are free to move around in the room.

6.1 Architecture of MUD Tracking System

MuD has a simple architecture of three major steps in Fig. 5. First, it derives the hardware-dependent parameter c by any of the three proposed methods in Sec.5.2, (i.e., specifications, chamber or online training). In the run-time, a number of anchors with given positions will function as the receivers to receive beacon messages from the target node (transmitter). Anchor nodes collect the RSS measurements, alter their channels of the measurements (transmitter will also alter) and deliver the measurement results to a central server. The server will apply a trilateration algorithm and display the results. Typically, the first step conducts only once while the later two steps will keeping operating to provide the trace of the target.

6.2 Practical Challenges

During the implementation of MuD, we encounter some practical challenges. The first challenge is to guarantee frequency rendezvous for transmitters and receivers as we need RSS information from all the channels. To solve this problem, we perform synchronization for all the nodes by the reference-broadcast method [9]. At first, all the nodes will be synchronized at the same channel. After certain period of time, all the nodes will switch to another channel until all the channels are visited and measured.

A second challenge is to avoid beacons collisions among nodes since collisions may corrupt the RSS measurements. To avoid such collisions, all the anchors nodes are merely the receivers and simply receive the beacon messages. The target node will be the only transmitter that sends out beacon messages. When there are multiple target nodes to be localized and tracked, simple scheduling approach can help to avoid collisions. Notice that one packet is sufficient to measure the RSS, and the current PHY layer protocols can easily support up to hundreds of packets per second without severe collisions.

To avoid radio interference from external sources, we turn off all the radio devices in the adjacent spectrums during the experiment. We use wired network to deliver the measurements from anchor nodes to the server to reduce the unnecessary wireless traffic and radio interference. As such, the measured RSS will be quite clean.

6.3 Implementations of MUD Tracking System

We implement MuD tracking system based on TelosB sensor platform [1] because of its low cost, easy implementation and convenient deployments, though our method has the general applicability to all RSS-based ranging and localization.

Fig. 6 shows the $20 \times 20m^2$ laboratory where MuD is deployed. Three anchor nodes are deployed at the corner of the ceiling of the laboratory. A snapshot of the system layout is depicted in Fig. 7.

At the transmitter and receiver ends, by the 802.15.4 standard TelosB sensors support the frequency ranging from $2.4 - 2.4835GHz$. This band is divided into 16 channels with $22MHz$ bandwidth for each and
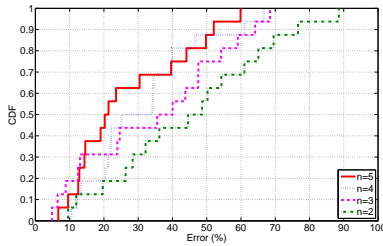
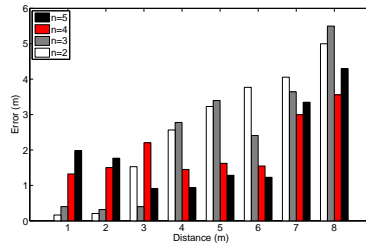Fig. 8. Accuracy of individual ranging with different path number (CDF)

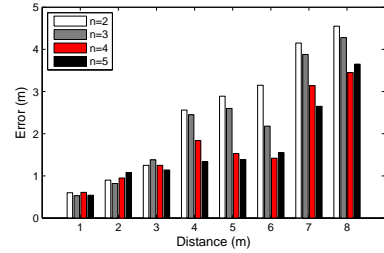Fig. 9. Accuracy of individual ranging with different path number

Fig. 10. Accuracy of individual ranging with different path number in a different lab

channels are spaced by $5MHz$. The wavelengths of these radio waves are on the order of centimeter and the wavelength of adjacent spectrums is around 0.03 centimeters. The transmission power is fixed at $-10dBm$.

In the second tracking step, we employ a simple slot-based scheduling algorithm for target nodes (transmitters). Each transmitter stays in one channel for about $50ms$ to send out beacons. When the anchor nodes receive these packets, it means the target enters the system. They will immediately transmit the data back to the server. To reduce unnecessary wireless traffic and radio interference, anchor nodes are connected to the server through USB cables. As long as the transmission of beacon message is over, transmitters and receivers will switch to a new channel for the next measurements. When all the channels have been visited once, the server begins to track. In our system, 16 channels are employed to measure which will introduce around 0.8 second tracking delay.

Upon the arrival of the RSS measurements, the server begins its computation. As the analysis quickly converges to a solution, the computational and memory overhead is low. Therefore daily PCs with standard configurations will provide sufficient capability. In our system, except the Chamber training approach that requires the Chamber room, all the other devices are off-the-shelf-product.

After the ranging for each anchor node to the target node (transmitter), trilateration localization [31] is applied to achieve the target location on the ground. Traditional RSS-based localization technologies rarely use trilateration, since they are hardly to realize accurate ranging between two nodes. Applying MuD into trilateration is able to verify that the MuD method can realize accurate ranging without high cost, laborious training or other environmental limitations.

7 PERFORMANCE EVALUATION

In this section, we evaluate the MuD method and tracking system based on implemented experiments. We first investigate the impacts of the various factors in the design and then evaluate the performance of MuD tracking system. Notice that all our experiments

are conducted in dynamic environments by default where several people (typically five) are free to move around in the room.

7.1 The Impact of Assumed Multipath Number

In the first set of experiments, we investigate the impacts of the number of paths n in the model function $P(x, \lambda)$ on the ranging accuracy.

Our experiment is based on one fixed pair of sensors. We conduct the experiments under 32 different distances ranging from $1m$ to $8m$ with $0.25m$ apart. In the analysis, the number of paths n varies from 2 to 5. In these experiments, the parameter is obtained by online training. The initial value of d_1 is set as 1 and the other initial values are set according to Sec. 4.4.

Fig. 8 shows the cumulative density function (CDF) of normalized errors in percentage and Fig. 9 gives the absolute error value in meters. Here normalized error means that, each error value E is normalized as $\frac{E-E_{min}}{E_{max}-E_{min}}$, where E_{min} is the minimal calculated error and E_{max} is the maximum calculated error. In general, we find $n = 5$ outperforms the other settings with over 65% of ranging having the ranging error less than 20%. we also find that when $n > 4$, the accuracy improvement is marginal. We may see that, $n = 2$ has the average ranging error about 45% and the average ranging errors of $n = 4$ and $n = 5$ are almost the same (about $23\% - 25\%$).

The reason is that in practice we have no knowledge of n and can only make assumption on it to carry out the analysis. A high n will introduce more variables to the model function $P(x, \lambda)$, which risks the problem become ill-conditioned during the computation. In addition, we also find that, when the node distance is very short (e.g., less than $2m$), lower n will have a relative higher accuracy. It may because in that scenario the actual number of paths is small too.

To further investigate the impact of assumed multipath number, we performed another experiment in a different environment (a different lab). We tested over 40 different distances ranging from $1m$ to $8m$ with $0.25m$ apart. Fig. 10 shows the absolute error value in meters. We also find that $n = 5$ outperforms the other settings with average ranging error $1.74m$. However,
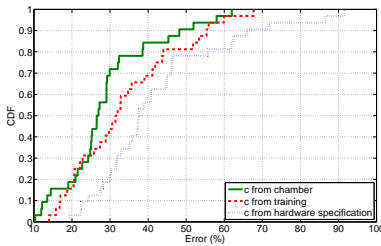
Fig. 11. Accuracy of individual ranging with different c (CDF)
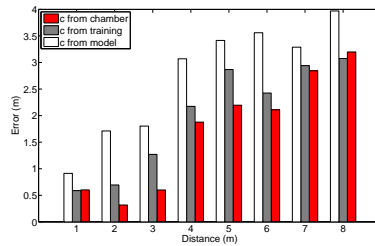
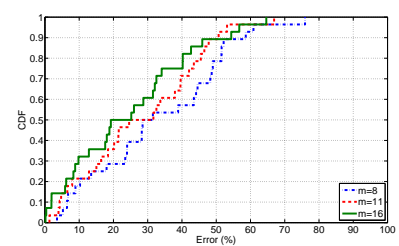Fig. 12. Accuracy of individual ranging with different c

Fig. 13. Accuracy of individual ranging with different channel number (CDF)

the average ranging difference between $n = 5$ and $n = 4$ setting is very small (only several centimeters).

Considering all these factors we set $n = 4$ in our later experiments.

7.2 The Impact of c

In this set of experiments we evaluate the different approaches to obtain the fixed unknown c, i.e. by hardware specifications, from chamber and from training. The experiment setting is the same as the above except $n = 4$.

The comparison results are shown in Fig. 11 and Fig. 12. Fig. 11 is the CDF of on the normalized errors from all samples, and Fig. 12 shows the absolute errors. We may see that the hardware specification approach performs the worst among others. Its average error is about 40%. We believe it is mainly due to the hardware derivation on this parameter. Not surprisingly, the chamber training approach performs the best accuracy (about 25%). We also find that the online training approach exhibits a similar performance as the ideal chamber training. The average error is about 30%. Compared with the chamber approach, the performance loss is only 5%.

In our later experiment, we apply the online training approach because of the practical concerns.

7.3 The Impact of Used Channel Numbers

Fig. 13 compares the normalized ranging accuracy with different channel numbers $m = 8, 11, 16$ respectively. The absolute values are shown in Fig. 14. We set $n = 4$, take the online training approach and the other settings are the same as above.

We find that, $m = 8$ has the averaged range error about 32%. When we use the maximum number of channels 16, the accuracy is the best 26% in average. Based on these, we suggest more channels when they are available when latency and measurement overhead are not the concern.

7.4 The Impact of Initial Value Setting in MuD

Initial value setting for iterations will also affect the final performance. To investigate its impacts, we test

different setting on LOS path length (d_i) in our experiment. The initial values of others will also be changed according to d_1. The other experimental settings are suggested as above experiments. The experiment results are shown in Fig. 15. According to the figure, the initial values have great impact on the accuracy. Especially when the initial value is very large, e.g., 50 times of the real sensor distance. Only when the initial value is set within a reasonable range (say several times of the real distance), a reasonable solutions will be expected. These confirm the importance of the online training. We should continuously track the target so that a reasonable estimation of the solutions can be set as the initial setting. Specifically, we continuously calculate the target position. Each time, we choose to use the previous tracking result as the initial value of current input in the real scenario. As the target has limited mobility in the indoor environments, this estimation will be close to the real one. The impact of initial value setting will be effectively alleviated. How to get a reasonable estimation when we have no any pre-knowledge of the target is left for future work.

7.5 Accuracy of Individual Distance Ranging

To comprehensively investigate our method for ranging, we conduct experiments between 20 pairs of nodes with 500 sample distances and the experimental results are shown in Fig. 16. We can see that by traditional ranging-based technology [30] (mapping the RSS information to distance directly), the average ranging error is around 300%. By our method, the average error decreases to about 30%, and the improvement is up to 10 times.

To explain how this happens, Fig. 16 further shows the RSS behaviors before and after distinguishing the multipath signals. We find that, before distinguishing, the RSS curve fluctuates dramatically as the distance grows due to the multipath effect. But after distinguishing, the multipath effects are successfully filtered out and the residual RSS from the LOS path becomes much smoother. It decreases nearly monotonically as the distance increases. Such results are much similar to the results of experiments in the ideal chamber room where multipath effect is not obvious. As Fig. 17
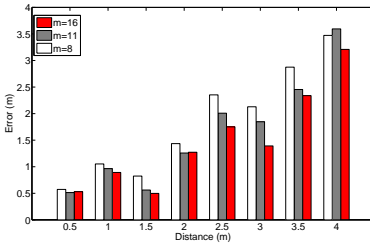
Fig. 14. Accuracy of individual ranging with different channel number
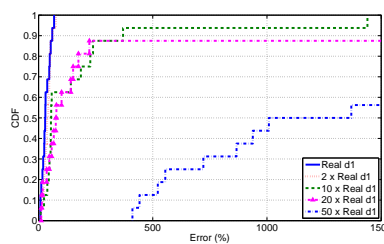

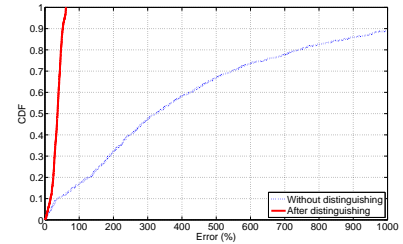Fig. 15. Accuracy of individual ranging with different initial value

Fig. 16. Accuracy comparison without/after filtering out multipath effect

shows, the difference between RSS after distinguishing and ideal RSS in chamber is only about 10%.

7.6 Accuracy of MuD Tracking System

In this subsection, we will evaluate the accuracy of the MuD tracking system. Fig. 18 shows our testbed in real experimental environment in a bird view. Three TelosB sensors are hung on the ceiling of the floor acting as the receivers (the shallow circles in Fig. 18). In our experiments, we let a person to carry the target sensor. The walking speed is about $2m/s$.

Fig. 18 shows one example of the real trace and the estimated trace by the MuD tracking system. The solid line is the real trace and the dashed line is the estimated one. The average tracking accuracy of this example is about $1.5m$. If the target moving speed is decreased to about $1m/s$, the accuracy is improved to about $1m$, another example is shown in Fig. 19. We tested 100 target traces on the ground. As Fig. 20 shows, the average error in MuD tracking is about $1m$. We will leave how to accurately localize very fast moving object in our future work.

7.7 Latency of MuD Tracking System

In the MuD tracking system, the latency depends on how much time for each sensor to sweep over all the channels. In our scenario, we have 16 channels. At each channel, one packet is transmitted. From empirical study, each TelosB sensor node takes $7ms$ average to transmit a packet of 51 bytes [1]. But in order to avoid beacon collision in a multiple object scenario, we prolongs the data transmission time to $50ms$. The transmitter can randomly transmit the packet within this time. The Channel switching is about $0.34ms$. The other data transmission time through wire connection and computation time can be neglected. As a result, for each sensor node to finish switching all the sensor nodes should be $(50 + 0.34) \times 16 \approx 0.8s$. So the total latency can be expressed as $T_d = (T_{switch} + T_{trans}) \cdot N_{channel}$. Here, T_{switch} is the channel switching time for each sensor node. T_{trans} is the time for one sensor node to transmit a packet. $N_{channel}$ is the number of channels used in the algorithm.

In summary, our system can reach the real time tracking latency to as fast as $0.8s$. Lower latency is expected with smaller measurement time.

7.8 Comparison with Static Environment

We also compare the results in dynamic environments and static environment. In the static environment, no one is allowed to move. In this comparison, 20 positions on the ground are set as the target locations as shown in Fig. 7. In the dynamic environment, the people walking around cause the RSS to vary dramatically as shown in Fig. 21. The largest RSS difference among the test samples is up to $25dB$. Fig. 22 shows the accuracy of MuD tracking system in both static and dynamic environments. We can see that, as the multipath induced by the moving people and dynamic environments are successfully filtered out, the accuracy in the dynamic environment is quite similar to the accuracy in the static environment. They both have the averaged error about 1 meter. The difference between them is less than 5%. Such result confirms that MuD is robust to the environment changes.

8 RELATED WORK

RSS-based ranging and localization used to be an active research area in literature. Since there is no simple mapping between the measured RSS and the corresponding distance, most of the existing works attempt to find the appropriate mapping. For example, RADAR [2] built a radio map for the environment and referred to this map during the localization. Madigan et.al. [17] exploited the RSS of a number of links to locate these nodes simultaneously, which helps to reduce the localization latency. LANDMARC [19] localize nodes by finding some reference nodes who has the similar RSS value with the target nodes. It hopes those reference nodes can provide valuable location information for the target. All these approaches are essential profile-based, i.e., to build a kind of RSS profile for the environment, and refer this profile later. The critical assumption is that this RSS profile will not change. In dynamic environments, however, this assumption is not true as new radio propagation paths
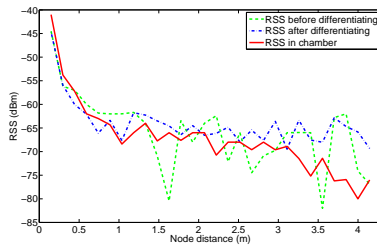
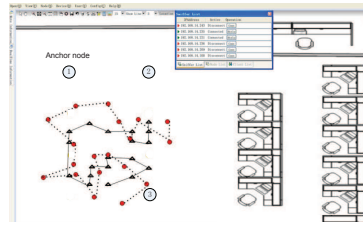Fig. 17. RSS results before and after differentiating

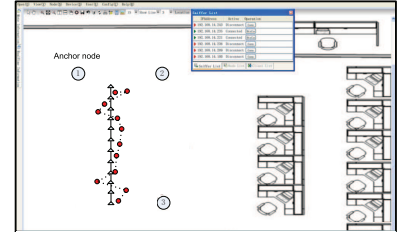Fig. 18. Tracking example 1

Fig. 19. Tracking example 2

may appear and existing paths may fade, causing the profile to change significantly.

Besides these deterministic approaches, probabilistic ones are also proposed (e.g., Horus [32], [11], [15], [29], [33]. In these approaches, a probabilistic model is constructed to represent the behavior of the link RSS values. We argue, however, the variance of the RSS values is not probabilistic. When the multi-path effects are correctly identified, RSS of wireless links are deterministic.

Indeed, the multi-path phenomenon not only affects the RSS-based ranging, but also affects other well-known localization mechanisms such as Angle-of-Arrival (AoA) [8], [16], Time-of-Arrival (ToA) [13], Time-Difference-of-Arrival (TDoA) [20], [22], light-based [27], and interferometric geolocation [18]. All these works assume that the signals are transmitted along the LOS path. In multipath environment, when the signals are from different paths towards the receiver, they all fail. It is noted that, although RIPS and related systems [18], [14], [4] can offer accurate ranging between two nodes, they all suffer from the multipath environments especial indoors.

An important related work is proposed by Rallapalli et.al [23]. They noticed the frequency diversity of RSS measurement but simply used the average to represent the RSS. In fact, all the RSS values at the different frequencies are correct. The difference exists because the changed constructive/destructive relations between signals from different paths. That difference is not because of the measurement errors. Noticing this, we use equations to explore such relations and get a better understanding of the multi-path effects. CUPID [24] can accurately estimate the angle and distance of a mobile device from a wireless access point. It requires multiple antennas to get the physical layer information CSI. Our work has no such requirement. We only utilize RSSI information and single antenna. It can be widely used for those common wireless nodes without any special hardware requirement.

In the communication community, the multipath effects have also been studied. A multi-carrier technology [6] use OFDM [5] technology to extract the phase information of the radio waves. It however needs the physical layer information and the cost is high. It is not suitable for commodity hardware.

In theory, both Rayleigh fading and Rician fading consider the combined impact of NLOS paths [26]. Rician fading occurs when typically there is a LOS path. Otherwise, Rayleigh fading occurs. They both contain a different random variable to simulate the signal variation in the multipath environments. However, our approach aims to differentiate the LOS signal from the combined arriving signals. For the radio propagation along each path, it is suitable to use the Friis model, by introducing the reflection coefficient.

9 DISCUSSION

MuD imposes minimal assumptions on the environment or the available hardware. Any transceivers with RSS measurement and frequency hopping capability are employable by MuD. In real environments, however, there are still some constraints that need further investigations.

First, besides the multi-path effect, another critical factor of the RSS measurement is the radio interference, especially from external radio sources. It may deviate the RSS values and even may cause the measurement to fail. In our experiments, we turn off all the background wireless traffic to avoid that impact, while in real environments, that effects are not ignorable. When the external interference is low, say constrained at certain spectrums, we can apply filtering algorithms when analyzing the RSS measurement and filter out the abnormal RSS measurements.

Second, MuD works when LOS between the targets and anchor nodes exist (not necessary to be the only). In some extreme case, the LOS may be blocked. This effect can be mitigated by designated deployment of anchors, while the tuned algorithm in the server to accommodate such situations also exist.

Third, in this paper we implement the localization and tracking for a single target. We employ the target transceiver as the transmitter and anchor nodes as receiver to minimize the tracking latency (currently it is less than 0.4 second). In real environments, the target may be many. A possible solution for this is to rotate the roles of the anchors and targets in RSS measurements. The anchors broadcast beacon messages, target
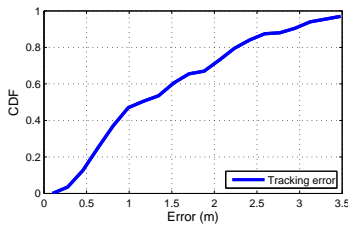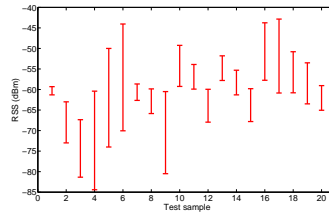
Fig. 20. Tracking error of MuD system

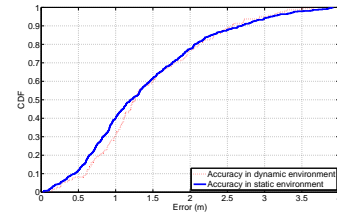Fig. 21. RSS variance in dynamic environment

Fig. 22. Tracking error in dynamic environment

nodes measure the RSS and transmit the results back to the central servers. This approach will experience more tracking latency. It will take the risk that the environment changes during the measurements, say the transceiver rotates and the orientation of nodes changes. These changes will cause MuD to fail.

10 CONCLUSION

In this paper, we study the multi-path phenomenon in RSS-based ranging and localizations. We propose to exploit the frequency diversity of the radio propagation paths to mine the phase information of the radio paths. As such, the signal amplitude of the LOS path can be identified. Applying the simple free-space model, rely only on the RSS measurements we can accurately ranging and localize nodes in dynamic environments with severe multipath effects. Experimental results show the ranging and localization errors are within one meter in average in a $20m \times 20m$ laboratory. Compared with the traditional RSS-based ranging approaches, the improvement is up to 10 times. The future work can be conducted according to Sec. 9. We will address the external radio interference issue when the interference is light. We will also study the scenarios when LOS path does not exist. At last, we will investigate techniques to accommodate changes of the environments during the RSS measurements, assuming that change exists but not significant.

ACKNOWLEDGMENTS

REFERENCES

[1] http://www.xbow.com/products/productdetails.aspx?sid=252. XBOW Corporation TelosB mote specifications.

[2] P. Bahl and V. N. Padmanabhan. Radar: an inbuilding rf-based user location and tracking system. In *Proceedings of IEEE InfoCom*, 2000.

[3] C. A. Balanis. Antenna theory: Analysis and design. In *2d Ed, Wiley: New York, NY*, 1997.

[4] H. Chang, J. Tian, T. Lai, H. Chu, and P. Huang. Spinning beacons for precise indoor localization. In *Proceedings of ACM SenSys*, 2009.

[5] S. Coleri, M. Ergen, A. Puri, and A. Bahai. Channel estimation techniques based on pilot arrangement in ofdm systems. In *IEEE Transactions on Broadcasting*, 2002.

[6] D. Cyganski, J. Orr, and W. R. Michalson. A multi-carrier technique for precision geolocation for indoor/multipath environments. In *Proceedings of IEEE ION*, 2006.

[7] J. J. E. Dennis and R. B. Schnabel. *Numerical Methods for Unconstrained Optimization and Nonlinear Equations*. 1996.

[8] E. Elnahrawy, J.-A. Francisco, and R. P. Martin. Bayesian localization in wireless networks using angle of arrival. In *Proceedings of ACM SenSys*, 2005.

[9] J. Elson, L. Girod, and D. Estrin. Fine-grained network time synchronization using reference broadcasts. In *Proceedings of OSDI*, 2002.

[10] X. Guo, D. Zhang, K. Wu, and L. M. Ni. Modloc: Localizing multiple objects in dynamic indoor environment. In *Proceedings of IEEE TPDS*, 2014.

[11] A. Haeberlen, E. Flannery, A. M. Ladd, A. Rudys, D. S. Wallach, and L. E. Kavraki. Practical robust localization over large-scale 802.11 wireless networks. In *Proceedings of ACM MobiCom*, 2004.

[12] S. N. Jasperson and S. E. Schnatterly. An improved method for high reflectivity ellipsometry based on a new polarization modulation technique. In *Review of Scientific Instruments*, 1969.

[13] B. Kusy, P. Dutta, P. Levis, M. Marotia, A. Ledeczi, and D. Culler. Elapsed time on arrival: a simple and versatile primitive for canonical time synchronisation services. In *International Journal of Ad Hoc and Ubiquitous Computing*, 2006.

[14] B. Kusy, A. Ledeczi, , and X. Koutsoukos. Tracking mobile nodes using rf doppler shifts. In *Proceedings of ACM SenSys*, 2007.

[15] A. Ladd, K. E. Bwkris, and A. Rudys. Robotics-based location sensing using wireless ethernet. In *Proceedings of ACM MobiCom*, 2002.

[16] J. Litva, A. Ghaforian, and V. Kezys. High-resolution measurements of aoa and time-delay for characterizing indoor propagation environments. In *IEEE Antennas and Propagation Society International Symposium*, 1996.

[17] D. Madigan, E. Elnahrawy, R. P. Martin, W. Ju, P. Krishnan, and A. Krishnakumar. Bayesian indoor positioning systems. In *Proceedings of IEEE InfoCom*, 2005.

[18] M. Maroti, B. Kusy, G. Balogh, P. Volgyesi, A. Nadas, K. Molnar, S. Dora, , and A. Ledeczi. Radio interferometric geolocation. In *Proceedings of ACM SenSys*, 2005.

[19] L. M. Ni, Y. Liu, Y. C. Lau, and A. P. Patil. Landmarc: Indoor location sensing using active rfid. In *Proceedings of IEEE PerCom*, 2003.

This article has been accepted for publication in a future issue of this journal, but has not been fully edited. Content may change prior to final publication. Citation information: DOI 10.1109/TMC.2016.2579619, IEEE Transactions on Mobile Computing

15

[20] C. Peng, G. Shen, Y. Zhang, Y. Li, and K. Tan. Beepbeep: a high accuracy acoustic ranging system using cots mobile devices. In *Proceedings of ACM SenSys*, 2007.

[21] D. Pozar. Microwave engineering. In *Proceedings of 2nd ed., John Wiley and Sons, Inc.*, 1998.

[22] N. B. Priyantha, A. Chakraborty, and H. Balakrishnan. The cricket location-support system. In *Proceedings of ACM Mobi-Com*, 2000.

[23] S. Rallapalli, L. Qiu, Y. Zhang, and Y. Chen. Exploiting temporal stability and low-rank structure for localization in mobile networks. In *Proceedings of ACM MobiCom*, 2010.

[24] S. Sen, J. Lee, K.-H. Kim, and P. Congdon. Avoiding multipath to revive in building wifi localization. In *Proceedings of IEEE MobiSys*, 2013.

[25] P. Sharma and S. Tripathi. Node localization using received signal statistics. In *Proceedings of IEEE MASS*, 2005.

[26] B. Sklar. Rayleigh fading channels in mobile digital communication systems. In *IEEE Communications Magazine*, 1997.

[27] R. Stoleru, T. He, J. A. Stankovic, and D. Luebke. A high-accuracy, low-cost localization system for wireless sensor networks. In *Proceedings of ACM SenSys*, 2005.

[28] E. Z. W. N. Systems. Design with an inverted-f pcb antenna.

[29] T. Tonteri. A statistical modeling approach to location estimation. In *IEEE Transaction on Mobile Computing*, 2002.

[30] K. Whitehouse, C. Karlof, and D. Culler. A practical evaluation of radio signal strength for ranging-based localization. In *Proceedings of ACM SIGMOBILE*, 2007.

[31] Z. Yang and Y. Liu. Quality of trilateration: Confidence-based iterative localization. In *Proceedings of IEEE TPDS*, 2010.

[32] M. Youssef and A. Agrawala. The horus wlan location determination system. In *Proceedings of ACM MobiSYS*, 2005.

[33] M. A. Youssef, A. Agrawala, and A. U. Shankar. Wlan location determination via clustering and probability distributions. In *Proceedings of IEEE PerCom*, 2003.

[34] D. Zhang, Y. Liu, X. Guo, and L. M. Ni. Rass: A real-time accurate and scalable system for tracking transceiver-free objects. In *Proceedings of IEEE TPDS*, 2013.

[35] D. Zhang, K. Lu, R. Mao, Y. Feng, Y. Liu, Z. Ming, and L. M. Ni. Fine-grained localization for multiple transceiver-free objects by using rf-based technologies. In *Proceedings of IEEE TPDS*, 2014.

[36] D. Zhang, J. Ma, Q. Chen, and L. M. Ni. An rf-based system for tracking transceiver-free objects. In *Proceedings of IEEE PerCom*, 2007.

[37] D. Zhang and W. Zheng. Handbutton: Gesture recognition of transceiver-free object by using wireless networks. In *Proceedings of IEEE TIIS*, 2016.

Xiaonan Guo (guoxn@ust.hk) is currently working toward the PhD degree in the Department of Computer Science and Engineering at Hong Kong University of Science and Technology. His research interests include wireless sensor network, mobile computing. He is a member of the IEEE.

Min Gao (gao@ust.hk) is currently working toward the PhD degree in the Department of Computer Science and Engineering at Hong Kong University of Science and Technology. His research interests include wireless sensor network, mobile computing. He is a member of the IEEE.

Zhong Ming (mingz@ust.hk) received his Ph.D. in Computer Science from Zhong Shan University. He is now a full professor and vice dean at College of Computer Science and Software Engineering, Shenzhen University, China. His areas of interest include software engineering, the internet of things, distributed workflow management.

Lei Yang (leiyang@must.edu.mo) received her Ph. D degree in Mathematics from the Hong Kong University of Science and Technology, Hong Kong. She is currently an assistant professor of Faculty of Information and Technology in Macau University of Science and Technology. Her research interests include computational mathematics and related applications.

Yunhuai Liu (yunhuai.liu@gmail.com) received his Ph.D. degree in computer science and engineering from the Hong Kong university of Science and Technology, Hong Kong. He is currently a full professor of the Third Research Institute of Ministry of Public Security. His research interests include wireless sensor networks, pervasive computing and Networking and Distributed Systems.

Lionel M. Ni (ni@cse.ust.hk) is Chair Professor in the Department of Computer and Information Science and Vice Rector for Academic Affairs at the University of Macau. A fellow of IEEE and Hong Kong Academy of Engineering Science, Dr. Ni has chaired over 30 professional conferences and has received eight awards for authoring outstanding papers. He serves on the editorial boards of Communications of the ACM, IEEE Transactions on Big Data and ACM Transactions on Sensor Networks.

Dian Zhang (zhangd@szu.edu.cn) received her Ph.D. degree in computer science and engineering from the Hong Kong university of Science and Technology (HKUST), Hong Kong, in 2010. After that, she worked as a research assistant professor of Fok Ying Tung Graduate School, HKUST. She is currently an associate professor of Shenzhen University. Her research interests include wireless sensor networks, pervasive computing and Networking and Distributed Systems.